Journal of Neuroscience Methods 195 (2011) 111–115

Contents lists available at ScienceDirect

Journal of Neuroscience Methods

journal homepage: www.elsevier.com/locate/jneumeth

Short communication

# Optimal spectral tracking—Adapting to dynamic regime change

John-Stuart Brittain[a,*], David M. Halliday[b]

[a] Centre of Excellence in Personalised Healthcare, Institute of Biomedical Engineering, Department of Engineering Science, Old Road Campus Research Building, University of Oxford, Headington, Oxford OX3 7DQ, UK
[b] The Department of Electronics, The University of York, Heslington, York, North Yorkshire YO10 5DD, UK

ARTICLE INFO

*Article history:*
Received 14 October 2010
Received in revised form
12 November 2010
Accepted 21 November 2010

*Keywords:*
Spectral analysis
Kalman filter
Data-adaptive filtering
Time–frequency analysis

ABSTRACT

Real world data do not always obey the statistical restraints imposed upon them by sophisticated analysis techniques. In spectral analysis for instance, an ergodic process – the interchangeability of temporal for spatial averaging – is assumed for a repeat-trial design. Many evolutionary scenarios, such as learning and motor consolidation, do not conform to such linear behaviour and should be approached from a more flexible perspective. To this end we previously introduced the method of optimal spectral tracking (OST) in the study of trial-varying parameters. In this extension to our work we modify the OST routines to provide an adaptive implementation capable of reacting to dynamic transitions in the underlying system state. In so doing, we generalise our approach to characterise both slow-varying and rapid fluctuations in time-series, simultaneously providing a metric of system stability. The approach is first applied to a surrogate dataset and compared to both our original non-adaptive solution and spectrogram approaches. The adaptive OST is seen to display fast convergence and desirable statistical properties. All three approaches are then applied to a neurophysiological recording obtained during a study on anaesthetic monitoring. Local field potentials acquired from the posterior hypothalamic region of a deep brain stimulation patient undergoing anaesthesia were analysed. The characterisation of features such as response delay, time-to-peak and modulation brevity are considered.



## 1. Introduction

Analysis of biomedical data often involves the use of time-dependent frequency analysis, most commonly implemented as the short-time Fourier transform (STFT). The STFT is constructed as a concatenation of periodogram estimates, which in isolation are renowned for their poor statistical properties (Percival and Walden, 2000). This is often compensated by a repeat-trial philosophy where an ergodic process is assumed (Brillinger, 1981). Ergodicity is often inappropriate or even impractical in various circumstances. For instance, non-associative learning and consolidation are evolutionary processes that require numerous iterations—none of which can be considered the same. Anaesthetic monitoring is a 'single-shot' approach, precluding the use of a repeat-trial philosophy altogether. Here, we consider an extension of previous work relating to spectral tracking, and demonstrate its application for continuous monitoring.

The periodogram, whose variance is proportional to the square of the underlying spectrum, requires smoothing to attain consistency. Smoothing is commonly achieved by applying a data window, kernel smoothing in the frequency domain, or multitaper estimates (Thomson, 1982). In Brittain et al. (2009) we introduced a novel method of optimal spectral tracking (OST) that permits frequency-selective statistical inference across dissimilar length trials or continuous segmented data. Our approach was applied in the study of trial-varying parameters related to electromyographic recordings from human locomotion studies. Here, we extend the previously proposed method to incorporate data-adaptive spectral tracking. The form of tracking outlined in this report permits near instantaneous adaptation to dynamic regime change, maintained tracking of slow-modulating components and quick convergence providing desirable statistical properties.

## 2. Methods

### 2.1. Optimal spectral tracking

The original proposed method of spectral tracking provides a framework under which successive single-segment estimators may be smoothed to provide a statistically optimal estimate of the localised spectrum. Separate smoothing of the auto- and cross-spectra of a bivariate process permitted the evaluation of local coherence and phase information.

We consider a single-segment estimator to be the frequency domain transformation of a single epoch of data, estimated via

* Corresponding author. Tel.: +44 1865 234761; fax: +44 1865 272469.
*E-mail addresses:* john-stuart.brittain@eng.ox.ac.uk (J.-S. Brittain), dh20@ohm.york.ac.uk (D.M. Halliday).

0165-0270/$ – see front matter © 2010 Elsevier B.V. All rights reserved.
doi:10.1016/j.jneumeth.2010.11.017

the periodogram or multitaper approach. Under this restriction, the statistical characteristics of the estimate are known permitting the (transformed) frequency-domain ordinates to be tracked or smoothed in relation to some control parameter. In the original article, a dataset constituting variable speed locomotion was examined, where the control parameter was treadmill speed.

The single segment estimate (periodogram or multitaper spectrum) for a time-series $x$, epoch $m$, is denoted $P^{(m)}(f)$, evaluated at the Fourier frequencies $f_n = n/(N\Delta t)$ for $n = 1, \ldots, \lfloor N/2 \rfloor$, with $\Delta t$ the sampling interval. To ensure alignment at the Fourier frequencies, epochs are zero padded to some common length $N$ samples prior to processing. The elusive underlying spectrum for epoch $m$ is denoted $S^{(m)}(f)$. The estimated local spectrum, obtained through evaluation of the OST algorithm, is denoted $\hat{S}^{(m)}(f)$.

Single-segment estimates are then transformed, either using the logarithm (as in this paper) or through root evaluation (see Brittain et al., 2009 for further details). A Kalman filter is implemented to provide tracking over single-segment estimates. The Kalman filter provides the maximum likelihood estimate given state and measurement equations corrupted by additive Gaussian noise. Since our (transformed) single-segment estimators are approximately normal, we require only the mean and variance of $\ln(P^{(m)}(f))$ to permit tracking. In the case of the log-transform multitaper estimate, the variance is given by (Percival and Walden, 2000)

$$\mathrm{var}\{\ln P^{(m)}(f)\} = \psi'(L) \tag{1}$$

for $0 < f < 1/(2\Delta t)$ with $\psi'(L)$ the trigamma function. $L$ represents the number of segments making up the spectral estimate. When $f = \{0, 1/(2\Delta t)\}$ the variance becomes $\psi'(L/2)$. For the periodogram $L = 1$. For multitaper methods $L$ corresponds to the equivalent number of tapers utilised in the single-segment estimate (Brittain et al., 2009).

Following Brittain et al. (2009), we define the measurement vector

$$\boldsymbol{z}_k = [\ln P^{(k)}(f_0), \ldots, \ln P^{(k)}(f_{\lfloor N/2 \rfloor})] \tag{2}$$

with state-vector $\boldsymbol{x}_k$ similarly defined, replacing $P^{(k)}(f_n)$ with $\hat{S}^{(k)}(f_n)$.

Our state-space formulation is now outlined below,

$$\boldsymbol{x}_{k+1} = \boldsymbol{\phi}_k \boldsymbol{x}_k + \boldsymbol{w}_k \tag{3}$$

$$\boldsymbol{z}_k = \boldsymbol{H}_k \boldsymbol{x}_k + \boldsymbol{v}_k \tag{4}$$

In this study we wish to track the mean of the transformed spectral estimate and therefore set $\boldsymbol{\phi}_k = \boldsymbol{H}_k = \boldsymbol{I}$. The usual Kalman predict-update loop can then be evaluated producing a posterior estimate of $\boldsymbol{x}_k$, which can be manipulated to recover the maximum likelihood local spectral estimate (Brittain et al., 2009). For full coverage of the Kalman filter OST implementation, along with details of augmentation with Kalman smoothing and root-transform filtering, see Brittain et al. (2009). Process and measurement noise terms, $\boldsymbol{w}_k$ and $\boldsymbol{v}_k$, are assumed i.i.d. normal with distributions given by $\mathcal{N}(\boldsymbol{0}, \boldsymbol{Q})$ and $\mathcal{N}(\boldsymbol{0}, \boldsymbol{R})$, respectively. Measurement noise variance $\boldsymbol{R}$ corresponds to the variance of the single segment estimator, $\psi'(L)$. Only the state-noise covariace matrix $\boldsymbol{Q}$ then remains to tune tracking specificity.

### 2.2. Adaptive tracking

We now propose the inclusion of data-adaptive state-noise, augmenting the OST procedure to provide an algorithm capable of identifying dynamic regime change. The approach is based on Jazwinski's method (Jazwinski, 1969) which inflates the state-noise covariance matrix when the attained variance of the error exceeds that predicted by the model.

We begin by specifying the likelihood (termed evidence, usually presented as the log-evidence) of an incoming observation given the current system state, $p(\boldsymbol{z}_k) = \mathcal{N}(\boldsymbol{z}_k; \hat{\boldsymbol{x}}_{k-1}, \boldsymbol{R} + \boldsymbol{P}_{k-1})$. Here, $\boldsymbol{P}_k$ is the Kalman derived covariance matrix for state $\hat{\boldsymbol{x}}_k$. The prediction error of the filter can then be stated as,

$$\boldsymbol{e}_k = \boldsymbol{z}_k - \hat{\boldsymbol{x}}_{k-1} \tag{5}$$

Unlike our original formulation, where the state noise covariance was constrained to the time-invariant isotropic matrix $\boldsymbol{Q} = q \cdot \boldsymbol{I}$, here we relax this constraint and introduce a time dependency. The (time-dependent) state-covariance matrix $\boldsymbol{Q}_k$ can now be updated using

$$\boldsymbol{Q}_k = h(\boldsymbol{e}_k \boldsymbol{e}_k^{\mathrm{T}} - \boldsymbol{R}_k^{(\boldsymbol{Q}=0)}) \tag{6}$$

with $h(x)$ the heaviside step function

$$h(x) = \begin{cases} x & \text{if } x \geq 0 \\ 0 & \text{otherwise} \end{cases}$$

The Jazwinski algorithm adaptively inflates state-noise covariance $\boldsymbol{Q}_k$ when the attained error variance $(\boldsymbol{e}_k \boldsymbol{e}_k^{\mathrm{T}})$ exceeds the *a priori* prediction variance $\boldsymbol{R}_k^{(\boldsymbol{Q}=0)}$, which assumes zero state-noise, such that

$$\boldsymbol{R}_k^{(\boldsymbol{Q}=0)} = \boldsymbol{R} + \boldsymbol{P}_{k-1} \tag{7}$$

In isolation this point estimate is of little value (Jazwinski, 1969), however parameter $\boldsymbol{Q}_k$ can be smoothed to produce a conditioned running estimate. A simple approach is to update $\boldsymbol{Q}_k$ via an exponential decay procedure. The final expression for $\boldsymbol{Q}_k$ can then be written,

$$\boldsymbol{Q}_k = \alpha \boldsymbol{Q}_{k-1} + (1-\alpha) h(\boldsymbol{e}_k \boldsymbol{e}_k^{\mathrm{T}} - \boldsymbol{R}_k^{(\boldsymbol{Q}=0)}) \tag{8}$$

where $\alpha$ acts as a smoothing parameter, allowing the adjustment of tracking sensitivity to transient fluctuations and hence regime change. Since $\boldsymbol{Q}$ inflates when the model encounters unexpected observations (those possessing a low log-evidence), this variable also acts as a measure of system stability in the stationary case.

Confidence intervals follow Brittain et al. (2009), where empirical limits are utilised in this study. Briefly, confidence intervals are placed in the (variance stabilising) log-domain under the assumption of normality, taking posterior mean and covariance estimates from the OST evaluation. Intervals can be converted to frequency-domain ordinates as required.

### 2.3. Synthetic data

Surrogate data were constructed to demonstrate the spectral tracking and rapid change-point capacity of our proposed adaptive OST solution. The data constitutes a frequency-selective gradient incline (in the log-domain) and step-reset. The signal is then reversed to demonstrate homogenous tracking performance both towards and away from regions of low signal-to-noise ratios (SNR). Data of length $N$ samples were generated as realisations of the process $x_k = \mathcal{H}((\exp(s_k) - 1)n_k) + e_k$ where

$$s_k = \begin{cases} 0 & 0 < k \leq t_1 \\ (k - t_1)/(t_2 - t_1) & t_1 < k \leq t_2 \\ 1 & t_2 < k \leq t_3 \\ 0 & t_3 < k \leq t_4 \\ 1 & t_4 < k \leq t_5 \\ (t_6 - k)/(t_5 - t_6) & t_5 < k \leq t_6 \\ 0 & t_6 < k \leq t_7 \end{cases} \tag{9}$$

Noise sources $n_k$ and $e_k$ are defined i.i.d. normal with distributions given by $\mathcal{N}(0, 100^2)$ and $\mathcal{N}(0, 1)$, respectively. We assume unit sampling for convenience. The function $\mathcal{H}(\cdot)$ represents a narrowband filter, here implemented as an eighth-order Butterworth infinite-impulse response with centre frequency $f_c = 0.3$ Hz and fractional passband 0.04 Hz. Our resulting sequence $x_k$ therefore constitutes

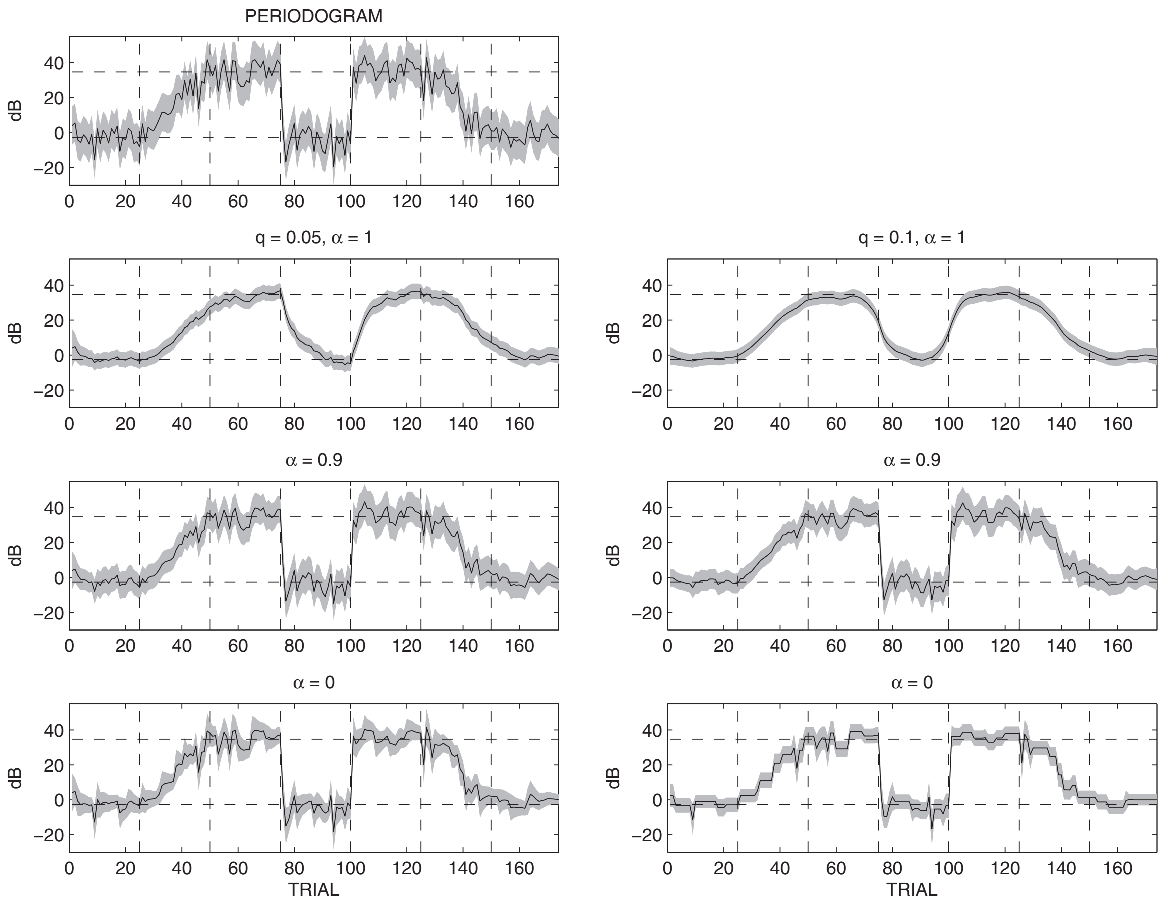


**Fig. 1.** OST applied to surrogate dataset. Top plot shows periodogram response to a frequency localised modulation in amplitude ($f = 0.3$ Hz). Left column: OST filtering (tracking) under varying $\alpha$; right column: OST smoothing under equivalent $\alpha$. Mean response shown with 95% confidence intervals about the mean. Dashed vertical lines denote changepoints in the surrogate dataset, as per Eq. (9). Dashed horizontal lines denote target analytic power levels at peak and baseline values. Dynamic OST estimates converge in a single step.

a narrowband modulating signal corrupted by broadband additive white noise. The sequence evolves in amplitude from baseline ($0 < k \leq t_1$) to log-linear incline ($t_1 < k \leq t_2$), plateau ($t_2 < k \leq t_3$) then step back to baseline. The sequence then reverses demonstrating the variance stabilising effect of spectral tracking towards high and low SNR states.

Data were generated with uniformly distributed change-points such that $(t_j - t_{j+1}) = 2.5 \times 10^4$ samples. Data were then segmented into epochs of 1000 samples and periodograms computed using a single (Gaussian) data taper. To demonstrate the convergence properties of spectral tracking we select the extreme case of an inconsistent estimator (the periodogram), while multitaper estimates remain equally applicable at this point. Our time-evolving spectrum now corresponds to the traditional short-time Fourier transform (STFT). OST routines were applied over periodogram ordinates to produce a sequence of conditioned estimates. Confidence intervals were computed empirically using the posterior covariance matrix.

### 2.4. Anaesthetic recordings

Anaesthetic data were acquired from a patient undergoing implantation of a pacemaker device for deep brain stimulation (DBS). Data were obtained with informed consent and under local ethics committee approval. DBS constitutes a neurosurgical procedure whereby stimulating macroelectrodes (Medtronic 3387) are implanted into deep regions of the brain and a continuous train of current pulses applied. The recordings presented in this paper were obtained from a patient suffering from cluster headache, which results in bouts of severe peri-orbital head pain. The electrode was implanted ipsilateral to head pain within the posterior hypothalamic region. Local field potentials (LFPs) were obtained continuously from the (externalised) DBS electrode as the patient was anaesthetised prior to implantation of the pacemaker.

## 3. Results

### 3.1. Synthetic data

Adaptive and non-adaptive OST algorithms were first applied to synthetic data (as described in Section 2.3). Fig. 1 shows frequency component $f = 0.3$ Hz from the surrogate dataset as evaluated through periodogram (STFT) and OST methods. We note immediately that the OST approach results in much smoother estimates that possess narrower confidence intervals and hence aid statistical inference. It is also evident from the non-adaptive approach that the underlying process model is violated on several occasions where an abrupt non-stationarity leads to a loss of specificity (i.e. slow-convergence).

For $\alpha = 1$ the adaptive OST estimate reverts to the traditional (non-adaptive) estimator. In this situation the choice of (isotropic) state-noise covariance matrix $\boldsymbol{Q} = q \cdot \boldsymbol{I}$ (specifying the $Q/R$ ratio) becomes critical. Manual tuning to equate the posterior variance with that attained through adaptive-OST results in a value of $q \approx 0.005$ (filtering) and $q \approx 0.01$ (smoothing). This leads to a severe degradation in tracking capacity (taking 21 steps to achieve signifi-

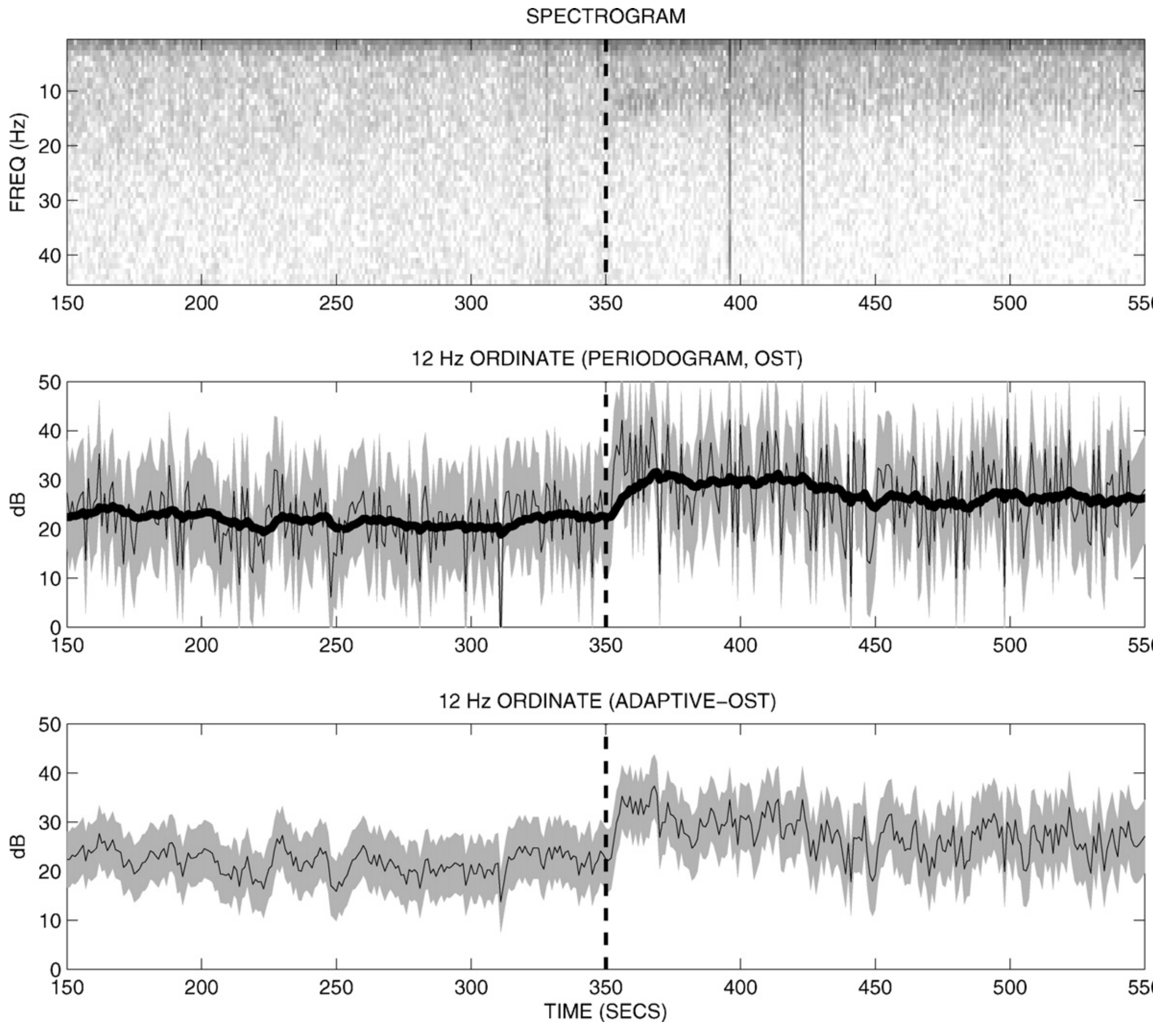


**Fig. 2.** Spectrogram of LFPs from anaesthesia recording (top). Middle plot shows the evolution of the 12 Hz ordinate from the spectrogram (periodogram ordinates together with 95% confidence interval represented by the thin line and shaded region, respectively) and OST (thick line) with process noise covariance $\boldsymbol{Q} = q \cdot \boldsymbol{I}$ taking $q = 0.01$. Bottom plot depicts adaptive-OST estimate with $\alpha = (1-10^{-3})$ (shaded region denotes pointwise 95% confidence intervals). The dashed vertical line in all plots represents the time of drug administration.

cant convergence in response to a step-change). In order to provide a reasonable level of tracking in this example, the state-noise variance was manually adjusted to $q = 0.05$ for filtering and $q = 0.1$ for smoothing. This represents an order of magnitude increase in assumed state-noise variance, permitting convergence in 14 steps (see Fig. 1). In the smoothed estimate, convergence occurs in an analogous 15 steps, this time centred about the transition point. For the adaptive OST approach, $\boldsymbol{Q}$ is initialized to zero and adjusted through the Jazwinski algorithm.

In comparing convergence with specificity we note that the periodogram estimate, under the variance stabilising logarithmic transform, produces 95% confidence intervals about the mean of 21.8 dB. Since the adaptive OST is necessarily data-dependent, confidence intervals will vary, however they attained a mean tracking level in this case of 16.7 dB for $\alpha = 0.9$ and 13.4 dB for $\alpha = 0$. The (manually adjusted) non-adaptive OST solution requires a time-invariant state-noise covariance and hence produces stable confidence intervals of 8.9 dB (for $q = 0.05$). Conversely, as confidence intervals shrink specificity is lost. In the extreme case of total adaptation ($\alpha = 0$), the gradient incline/decline results in a staircase effect as successive measurements force the process noise covariance to inflate under the (stationary) assumption of a static mean. This is clearly evident as a repeated convergence (and explosion) of confidence intervals in the tracking scenario.

We also note that relatively high smoothing levels can be attained by setting $\alpha = 0.9$ (elucidating smooth underlying modulations and potentially suppressing spurious extraneous noise) while maintaining sensitivity to change-points in the signal dynamics. In this example both step-changes in amplitude result in single-trial convergence of the local spectra, even in the (causal) tracking case.

### 3.2. *Anaesthetic recordings*

Prior to intubation a series of analgesic and hypnotic drug compounds were administered in preparation for surgery. Of particular interest in this report are the effects of propofol, fentanyl and magnesium which were administered together resulting in the rapid loss of consciousness of the patient. A modulation in LFP power was observed within the vicinity of the posterior hypothalamus at this time (see Fig. 2). Examination of the spectrogram appeared to demonstrate an increase in power at about 12 Hz. Evaluation of the time-course of this 12 Hz component (via periodogram ordinates) shows a highly variable signal evolving in time (Fig. 2). Due to the poor variance properties of the spectrogram however, this analysis leaves open to interpretation vital features of the anaesthetic response—specifically characterisation of the response delay, time-to-peak, modulation brevity (a fast transient effect versus a broader/slower synchronisation of the underlying neuronal population) and after-effect (for instance, time to return to baseline).

To address these issues we first apply the original non-adaptive OST algorithm, however this approach requires an *a priori* estimate of the state-noise covariance matrix. Since the state-noise covariance is assumed time-invariant within our model we are forced to select a *static* estimate that will determine the smoothness of the entire time-evolving spectrum. Since we assume no *a priori* knowledge relating to the expected smoothness of the anaesthetic response, we resort to assigning an arbitrary value to $\boldsymbol{Q}$. We therefore select $\boldsymbol{Q}$ as the isotropic matrix $\boldsymbol{Q} = q \cdot \boldsymbol{I}$ with $q = 0.01$. The (non-adaptive) OST solution is displayed with the periodogram estimate in Fig. 2. The OST estimate tracks a running mean through the periodogram ordinates, visibly reducing the variance of the estimate. On further inspect however we can consider this tracking too smooth since the increase in power immediately following drug administration does not respond quickly to the apparent step-like modulation visible from the periodogram approach. Indeed, due to the rapid power manifestation, several OST points (between 350 and 360 s) appear outside of the periodogram confidence intervals.

In applying the adaptive-OST methodology our state covariance converges to a data-driven equilibrium, capable of adapting to transient fluctuations in the underlying power dynamics. To prevent over-fitting in the presence of spurious noise we select adaptation rate $\alpha = (1 - 10^{-3})$. The result of applying our adaptive OST method to the anaesthetic data is presented in Fig. 2. While the estimate remains relatively smooth, the data-driven approach ensures inflation of the process noise covariance quickly in the presence of low evidence observations. The capacity to track slowly varying processes (after-effect in this case) while maintaining the ability to react to transient fluctuations (drug response) in a low variance environment demonstrates the real-world benefits of an adaptive OST approach.

## 4. Discussion

We have presented a powerful extension of a previous methodology, the OST framework, which aids data exploration with the potential to elucidate time-varying structure in paradigms where ergodicity is inappropriate. While much progress has recently been made in revealing the fine time–frequency microstructure of signals (e.g. Flandrin et al., 2003), these algorithms remain computationally costly, limiting their application to informed interrogation within small datasets. The OST approach provides a fast and efficient mechanism for data exploration, augmented by the newly formed adaptive OST.

In this extension to our previous work, we modify the OST routines to provide an adaptive implementation capable of identifying and reacting to dynamic transitions in the underlying system state. In so doing, we not only generalise our approach to encapsulate both slow-varying processes and rapid state transitions, but also provide a metric of system stability. Real-world application of the adaptive-OST approach was demonstrated in a dataset where a rapid modulation in frequency was observed in a high noise environment.

While we have chosen to demonstrate the adaptive capabilities of OST on a continuous data recording, the method remains amenable to the analysis of variable duration sequenced data (as demonstrated in the original study of Brittain et al., 2009). The adaptive solution is also amenable to the root-transform estimate (Brittain et al., 2009). Note however that since the variance of the root-transform is reliant upon an estimate of the underlying spectrum, the measurement noise covariance necessarily becomes data-dependent. Application of the adaptive OST will still improve performance in this case.

## Acknowledgements

This work was supported by The Centre of Excellence in Personalised Healthcare funded by the Wellcome Trust and EPSRC under grant number WT 088877/Z/09/Z. We wish to thank Dr. David Shlugman for his assistance in acquiring the anaesthetic data and Prof. Tipu Aziz for access to the patient. We also wish to thank Ned Jenkinson for assistance in data acquisition and manuscript preparation.

## References

Brillinger DR. Time series: data analysis and theory—expanded edition. CA: Holden Day; 1981.

Brittain JS, Catton C, Conway BA, Nielsen JB, Jenkinson N, Halliday DM. Optimal spectral tracking—with application to speed dependent neural modulation of tibialis anterior during human treadmill walking. J Neurosci Methods 2009;177:334–47.

Flandrin R, Auger F, Chassande-Mottin E. Time–frequency reassignment: from principles to algorithms. In: Papandreou-Suppappola A, editor. Applications in time–frequency signal processing, electrical engineering & applied signal processing series. FL: CRC Press; 2003. p. 179–203.

Jazwinski AH. Adaptive filtering. Automatica 1969;5:475–85.

Percival DB, Walden AT. Wavelet methods for time series analysis. Cambridge: Cambridge University Press; 2000.

Thomson DJ. Spectrum estimation and harmonic analysis. Proc IEEE 1982;70:1055–96.